

Self-assembly and Nanotechnology 10.524

Lecture 8. Nanofluids and Microfluidics

Instructor: Prof. Zhiyong Gu (Chemical Engineering
& CHN/NCOE Nanomanufacturing Center)

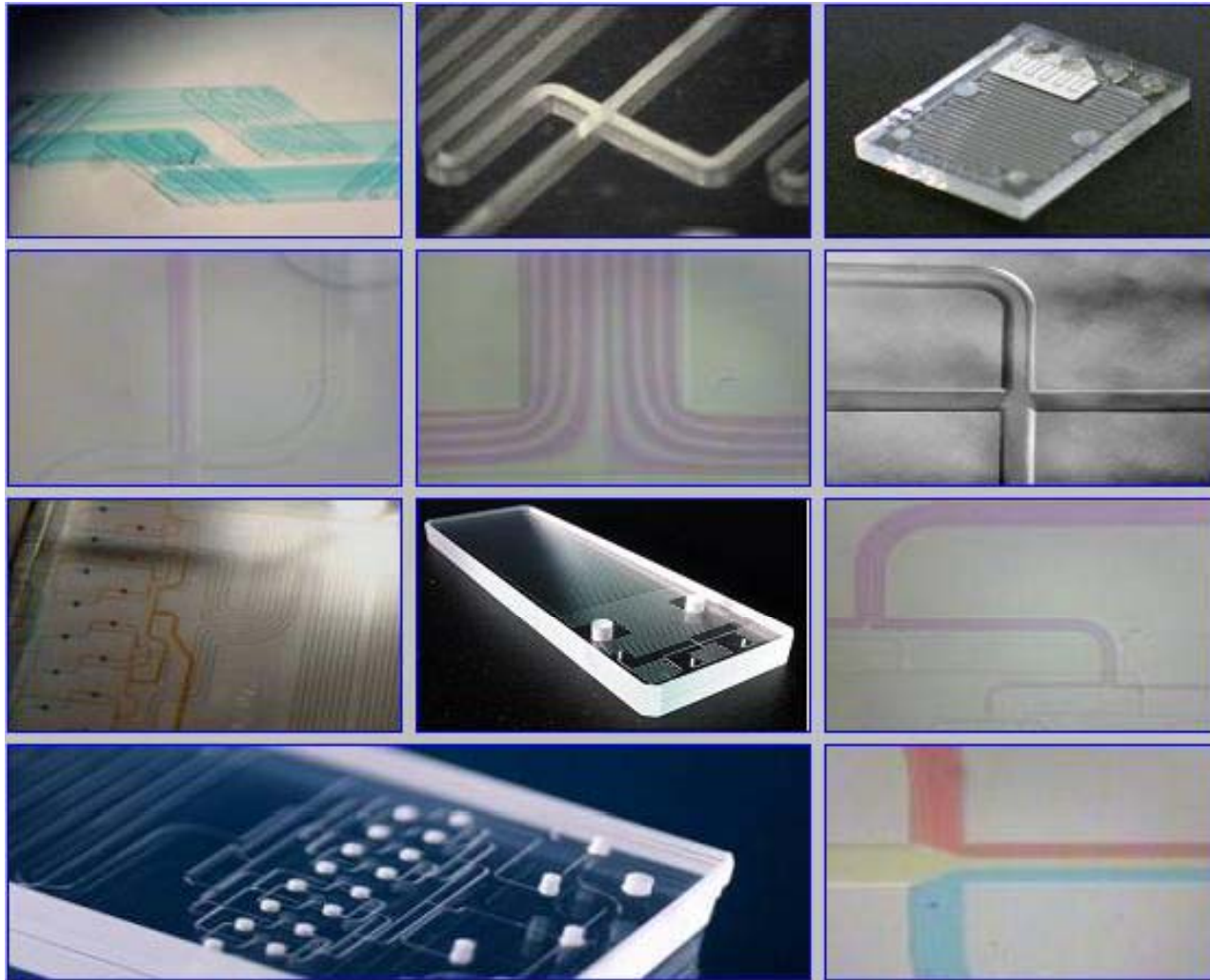
March 06, 2013

Microfluidics: Introduction

Microfluidics deals with the behavior, precise control and manipulation of microliter and nanoliter volumes of fluids. It is a multidisciplinary field comprising physics, chemistry, engineering and biotechnology, with practical applications to the design of systems in which such small volumes of fluids will be used. Microfluidics has emerged only in the 1990s and is used in the development of DNA chips, micro-propulsion, micro-thermal technologies, and lab-on-a-chip technology.

The behavior of fluids at the microscale can differ from 'macrofluidic' behavior in that factors such as surface tension, energy dissipation, and fluidic resistance start to dominate the system.

Microfluidics: Various Examples



Glass microfluidic devices from Syrris and Dolomite

Microfluidics

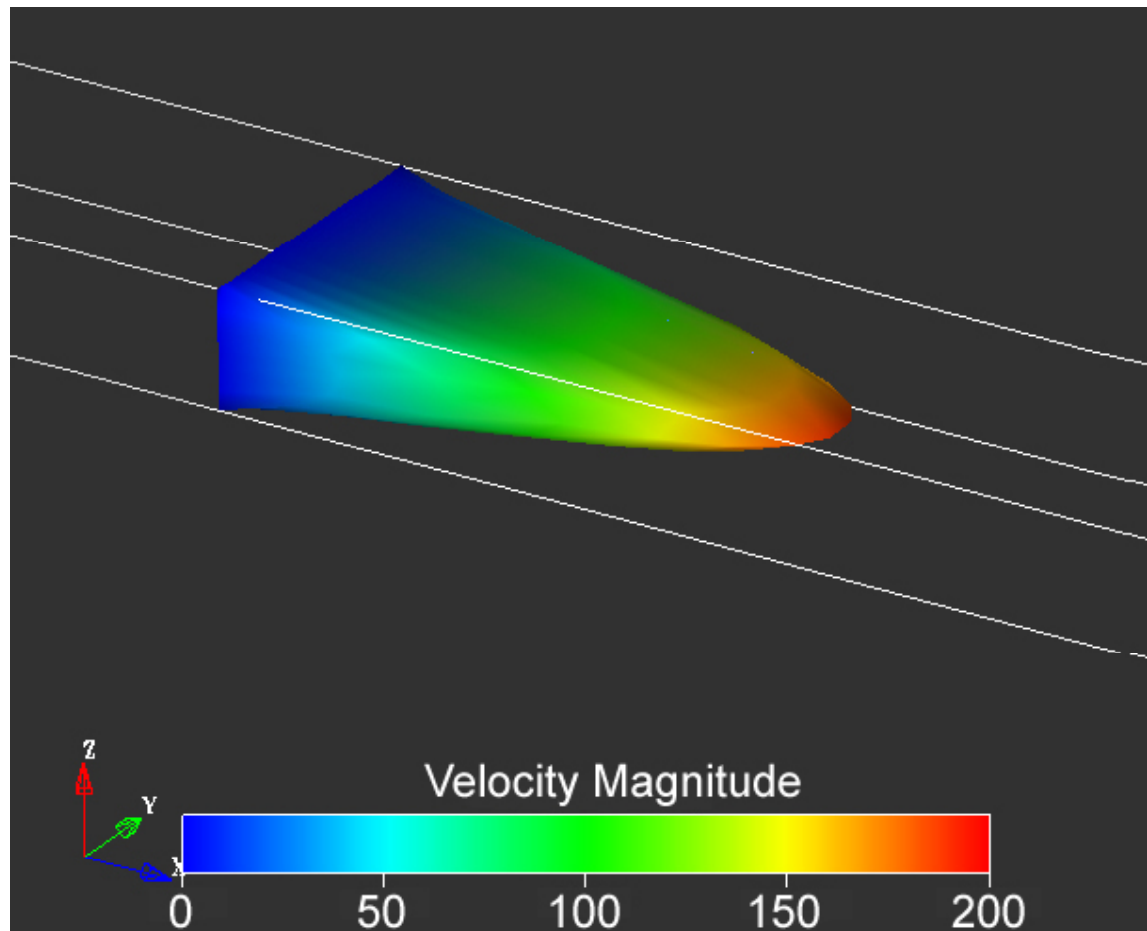
At small scales (channel diameters of around 10 to several hundred micrometers) some interesting and unintuitive properties appear. The Reynolds number, which characterizes the presence of turbulent flow, is extremely low, thus the flow will remain laminar. Thus, two fluids joining will not mix readily via turbulence, so diffusion alone must cause the two fluids to mingle.

Reynolds number is the ratio of inertial forces ($v_s\rho$) to viscous forces (μ/L) and consequently it quantifies the relative importance of these two types of forces for given flow conditions. Thus, it is used to identify different flow regimes, such as laminar or turbulent flow.

$$Re = \frac{\rho v_s L}{\mu} = \frac{v_s L}{\nu} = \frac{\text{Inertial forces}}{\text{Viscous forces}}$$

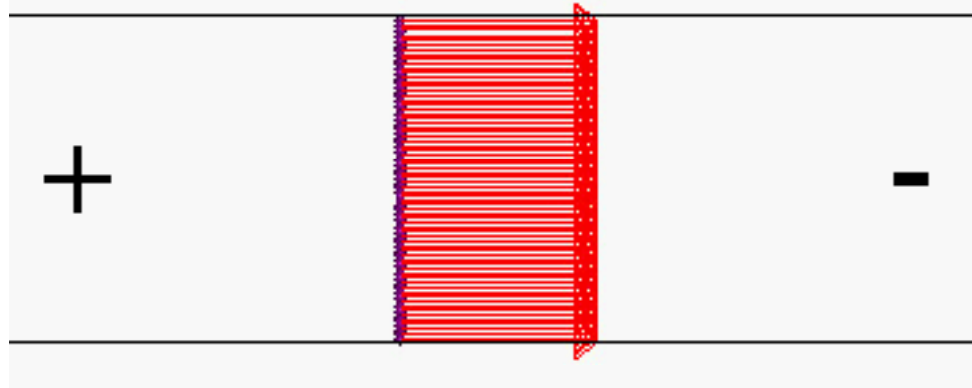
where: v_s - mean fluid velocity,
 L - characteristic length,
 μ - (absolute) dynamic fluid viscosity,
 ν - kinematic fluid viscosity: $\nu = \mu / \rho$,
 ρ - fluid density.

Microfluidics: Pressure Driven Flow



Velocity profile in a microchannel with aspect ratio 2:5 under conditions of pressure driven flow. Note that the velocity is assumed to be zero at the walls in most treatments of transport of liquids. Image from result of a calculation using Coventorware software.

Microfluidics: Electrokinetic Flow



The very interesting flow velocity profile calculated for electroösmotic pumping in an open channel. Such a channel (in the absence of backpressure) exhibits plug flow. Shown in the situation for negatively charged walls; the anode is at the left and the cathode is at the right. In fact the profile is very interesting close to the walls, since velocity drops to zero at the walls over a distance that is comparable to the thickness of the electrical double layer.

<http://faculty.washington.edu/yagerp/microfluidicstutorial/tutorialhome.htm>

Microfluidics: PDMS based



Photograph of a PDMS microfluidic device. It consists of a flat glass plate onto which has been deposited a gold layer in the form of two electrodes. The upper portion of the device was formed by PDMS that was formed on a mold that consisted of a flat Si surface that had been etched to leave a ridge in the form of an H-filter (3 ports in, 2 ports out). The 5 pieces of PDMS tubing used for fluidic access was set into the device prior to curing. Note that the clarity of PDMS makes it an excellent material for microscopic observation of processes in the microchannels.

<http://faculty.washington.edu/yagerp/microfluidicstutorial/tutorialhome.htm>

Microfluidics: Various Templates

Material:	Fabrication Technique:
Silicon	Chemical wet etch
Glass	Chemical etch, laser cutting
Polymeric films (e.g., Mylar)	Laminate laser cutting
Silicone elastomer (PDMS)	Micromolding ("soft lithography")
Photoresist, hydrogels, etc.	Photopolymerization ("microfluidic tectonics")
Thermoplastic	Hot embossing, injection molding

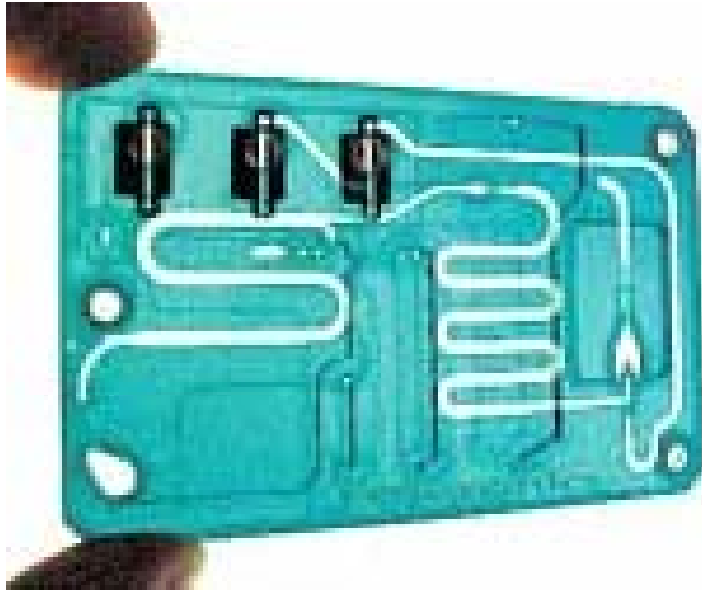
<http://faculty.washington.edu/yagerp/microfluidicstutorial/tutorialhome.htm>

Microfluidics: Applications

Advances in microfluidics technology are revolutionizing molecular biology procedures for enzymatic analysis (e.g., glucose and lactate assays), DNA analysis (e.g., polymerase chain reaction and high-throughput sequencing), and proteomics. The basic idea of microfluidic biochips is to integrate assay operations such as detection, as well as sample pre-treatment and sample preparation on one chip.

An emerging application area for biochips is clinical pathology, especially the immediate point-of-care diagnosis of diseases. In addition, microfluidics-based devices, capable of continuous sampling and real-time testing of air/water samples for biochemical toxins and other dangerous pathogens, can serve as an always-on "bio-smoke alarm" for early warning.

Microfluidics: Applications



Placing a drop of blood on this integrated disposable circuit of various microfluidic elements allows a white blood cell count that might need to be monitored in the event of chemical or biological warfare.
(Micronics, Inc.)



Quantitative gene expression results using a polymerase chain reaction can be obtained with this microfluidic card by pipetting in reaction mixes, centrifuging, sealing, removing the reservoir, and thermal cycling.
(Applied Biosystems)

<http://www.aip.org/tip/INPHFA/vol-9/iss-4/p14.html>

Microfabricated catalytic reactors

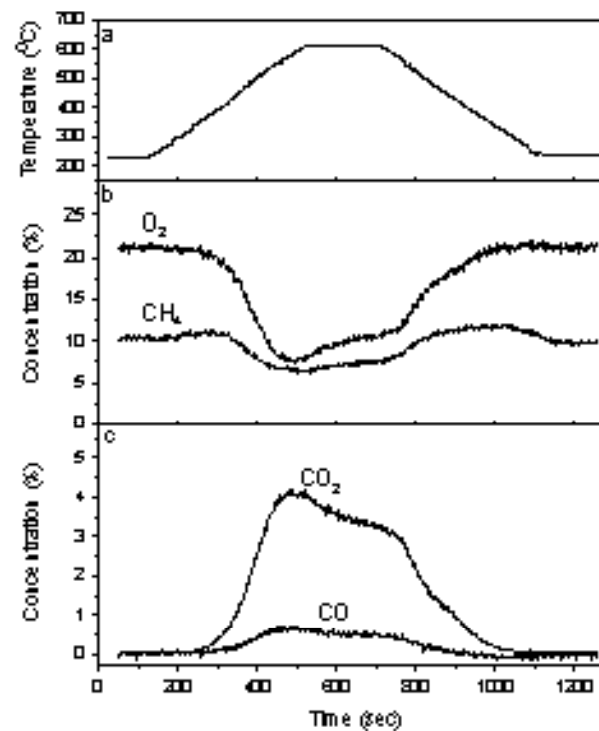
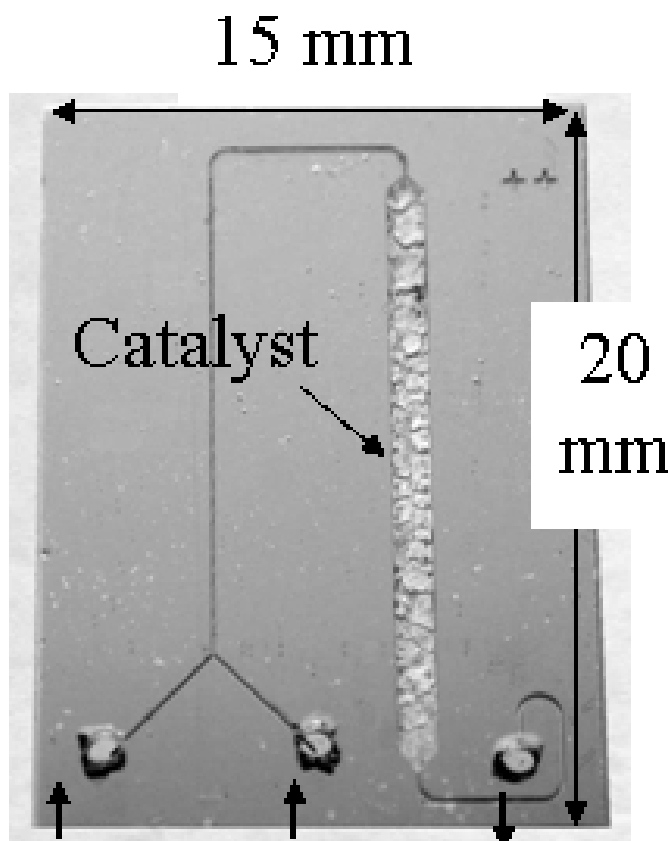


Fig. 4. Full oxidation reaction: (a) temperature ramp; (b) outlet concentrations of CH₄ and O₂; (c) outlet concentrations of CO₂ and CO. Total flow rate 4, 0.4 mL/min CH₄, 0.8 mL/min O₂ and 2.8 mL/min Ar.

Full and partial oxidation of methane over a palladium catalyst is studied in a microreactor at non-diluted gas mixtures. The explosive gas of methane and oxygen is mixed on the chip making the system completely safe due to the small volume.

O. Younes-Metzler, J. Svagin, S. Jensen, C. H. Christensen, O. Hansen, and U. J. Quaade, *Microfabricated high temperature reactor for catalytic partial oxidation of methane*, *Appl. Catal. A General* **284**, 5 (2005)

Microfabricated catalytic reactors (Cont.)

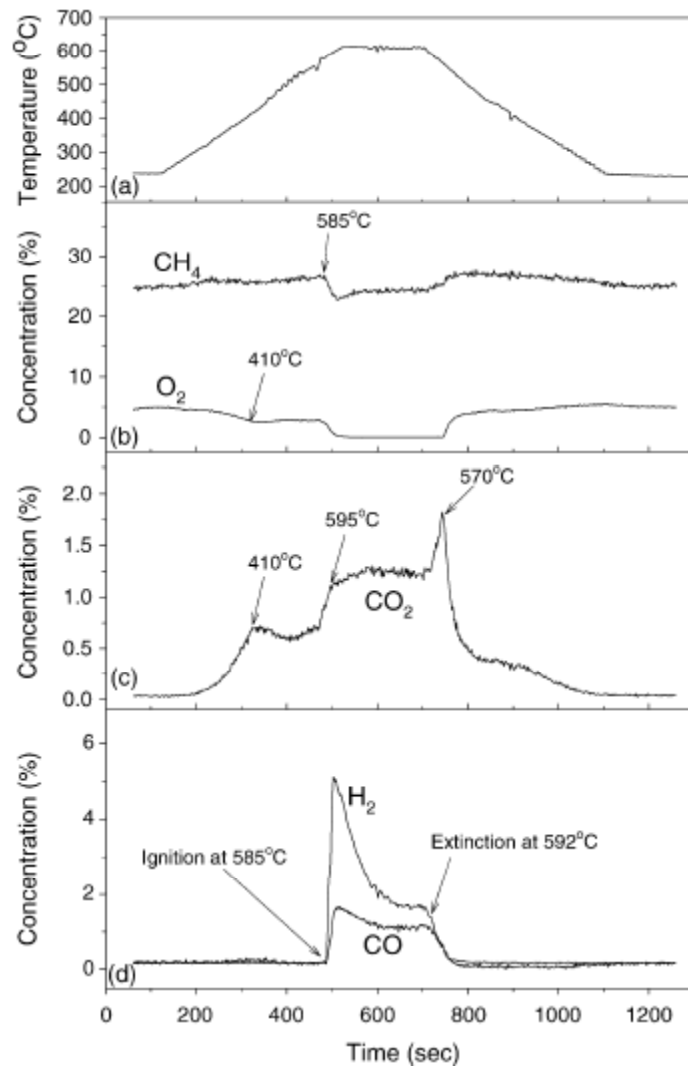


Fig. 6. Partial oxidation reaction: (a) temperature ramp; (b) outlet concentrations of CH_4 and O_2 ; (c) outlet concentrations of CO_2 ; (d) outlet concentrations of CO and H_2 . Total flow rate 4, 1.0 mL/min CH_4 , 0.2 mL/min O_2 and 2.8 mL/min Ar.

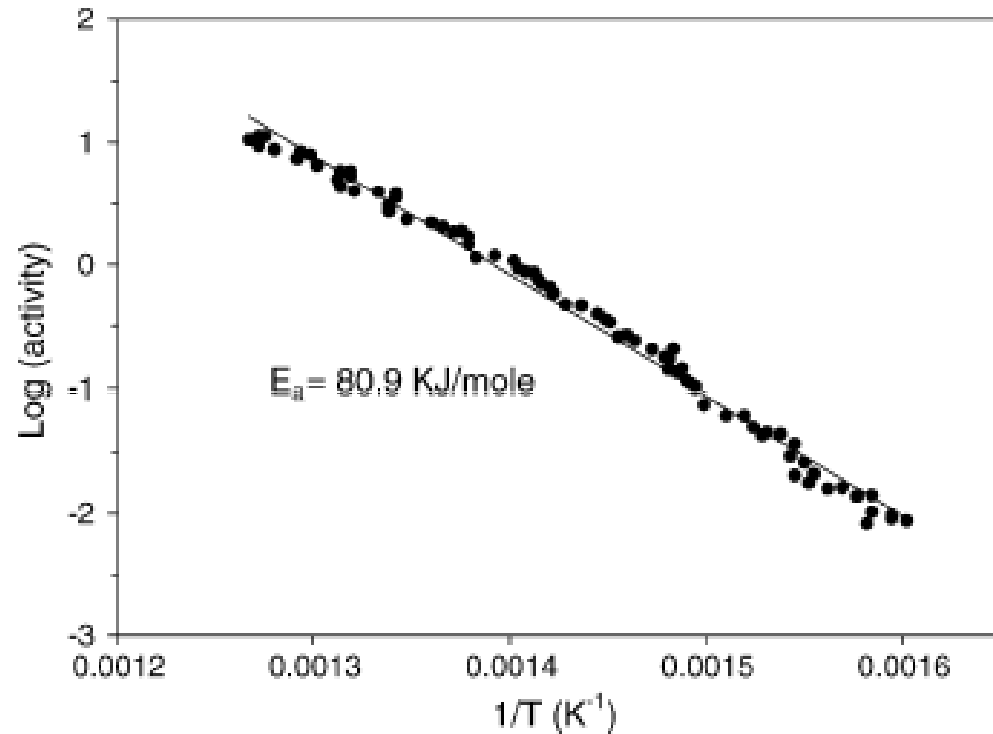


Fig. 5. Arrhenius plot based on the CO_2 signal.

Full and partial oxidation of methane over a palladium catalyst is studied in a microreactor at non-diluted gas mixtures. The explosive gas of methane and oxygen is mixed on the chip making the system completely safe due to the small volume.

Synthesis of Nanomaterials

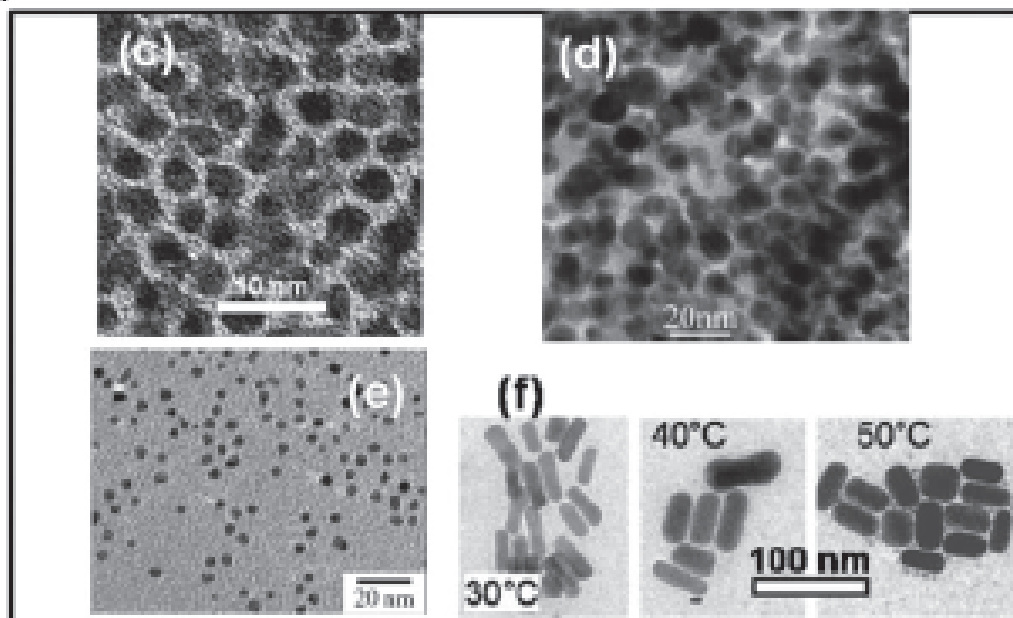
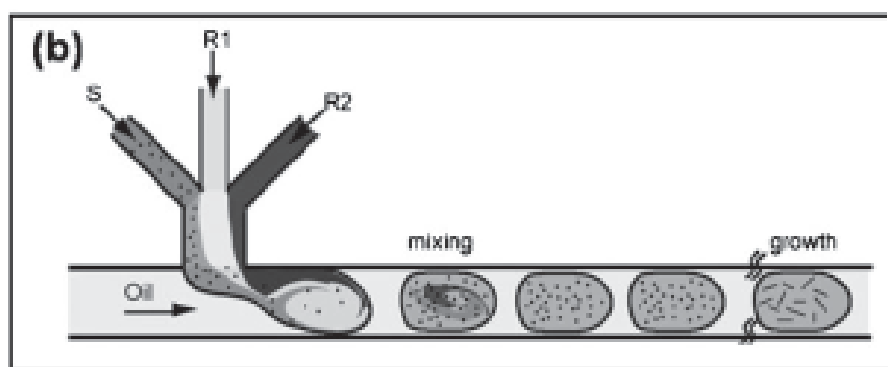
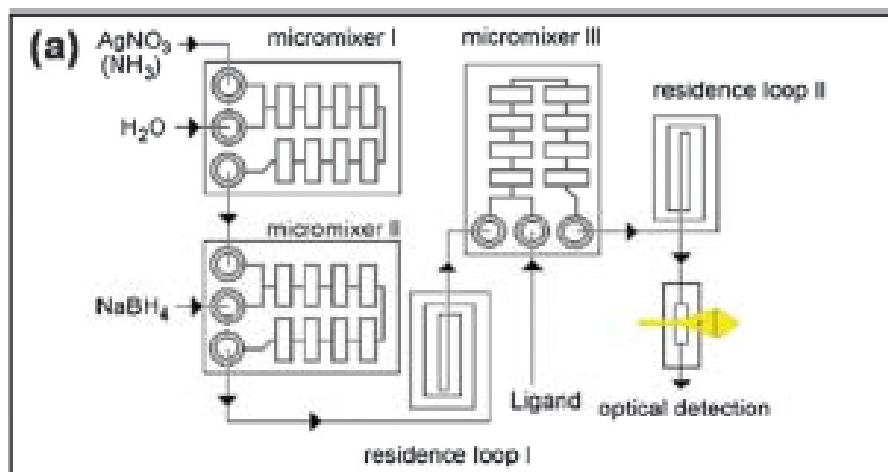


Fig. 8 General strategies for (a) the homogeneous synthesis of metal nanoparticles (*reprinted from ref. 108 with permission from Elsevier*) and (b) the droplet-based synthesis of nanorods (*Copyright Wiley-VCH Verlag GmbH & Co. KGaA. Reproduced with permission from ref. 123*). Examples of metal nanoparticles generated in microreactors. (c) gold nanoparticles (*reprinted from ref. 121 with permission from Elsevier*), (d) copper nanoparticles (*reprinted with permission from ref. 111. Copyright 2005 American Chemical Society*), (e) palladium nanoparticles (*with kind permission from Springer Science + Business Media ref. 126*), and (f) gold nanorods synthesized at different temperatures (*reproduced by permission of the PCCP Owner Societies*).¹²⁴

Microreactors and Microfluidic Channels for Microstructures

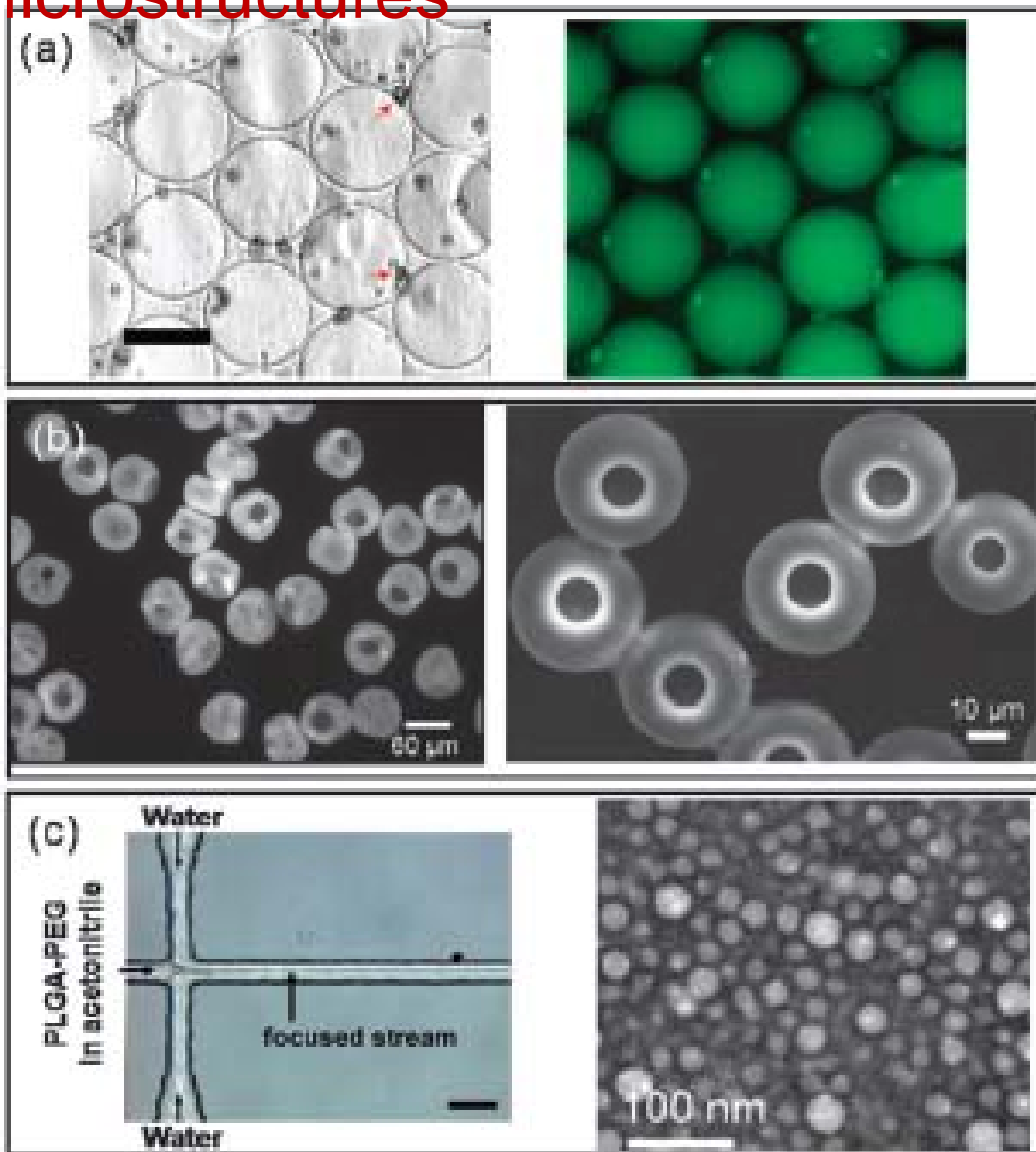


Fig. 6 Microstructures obtained using precipitation of polymer in microfluidic systems. (a) polymersomes from evaporation of the intermediate phase of a water/oil/water double emulsion (b) toroidal microparticles from the solvent removal by dissolution of a single emulsion in a PDMS/Glass microreactor (c) liquid/liquid micro antisolvent process for the synthesis of PLGA-PEG nanoparticles from acetonitrile-water flow focusing microreactor.

S. Marre and K.F. Jensen, *Chem. Soc. Rev. (RSC)*, **39**, 1183 – 1202 (2010)

Microreactors and Microfluidic Channels for Microstru

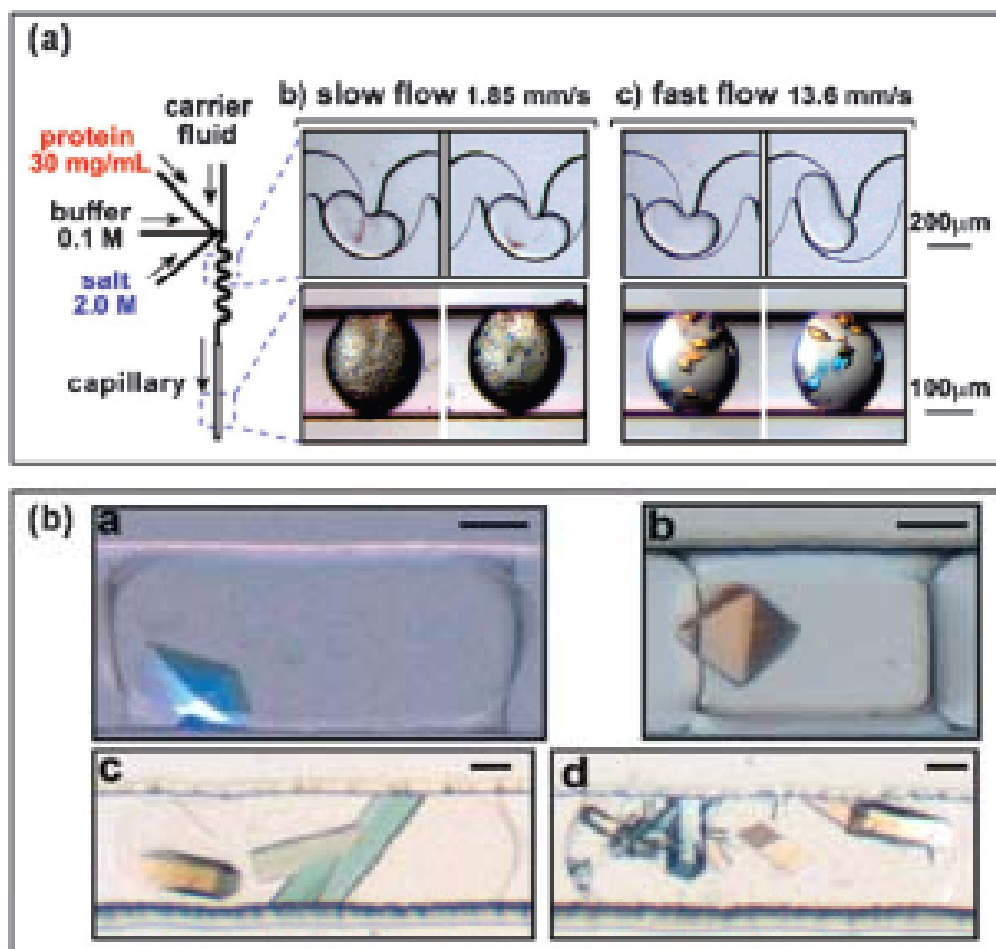
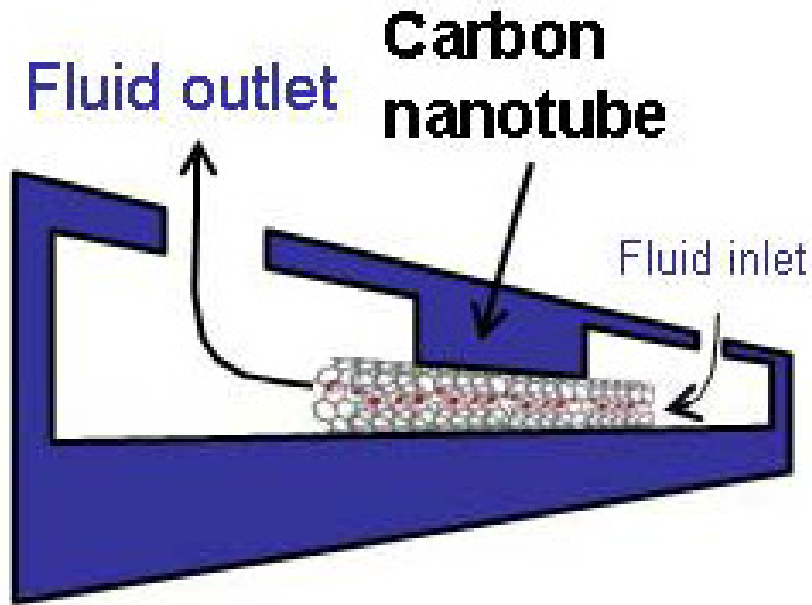


Fig. 7 (a) Example of proteins crystallization droplets-based microfluidic platform, for studying the effect of mixing. (b) Different proteins crystallized within slugs—Thaumatin, bovine liver catalase and glucose isomerase (*reprinted with permission from ref. 98 and 99, respectively. Copyright 2003 and 2005 American Chemical Society*).

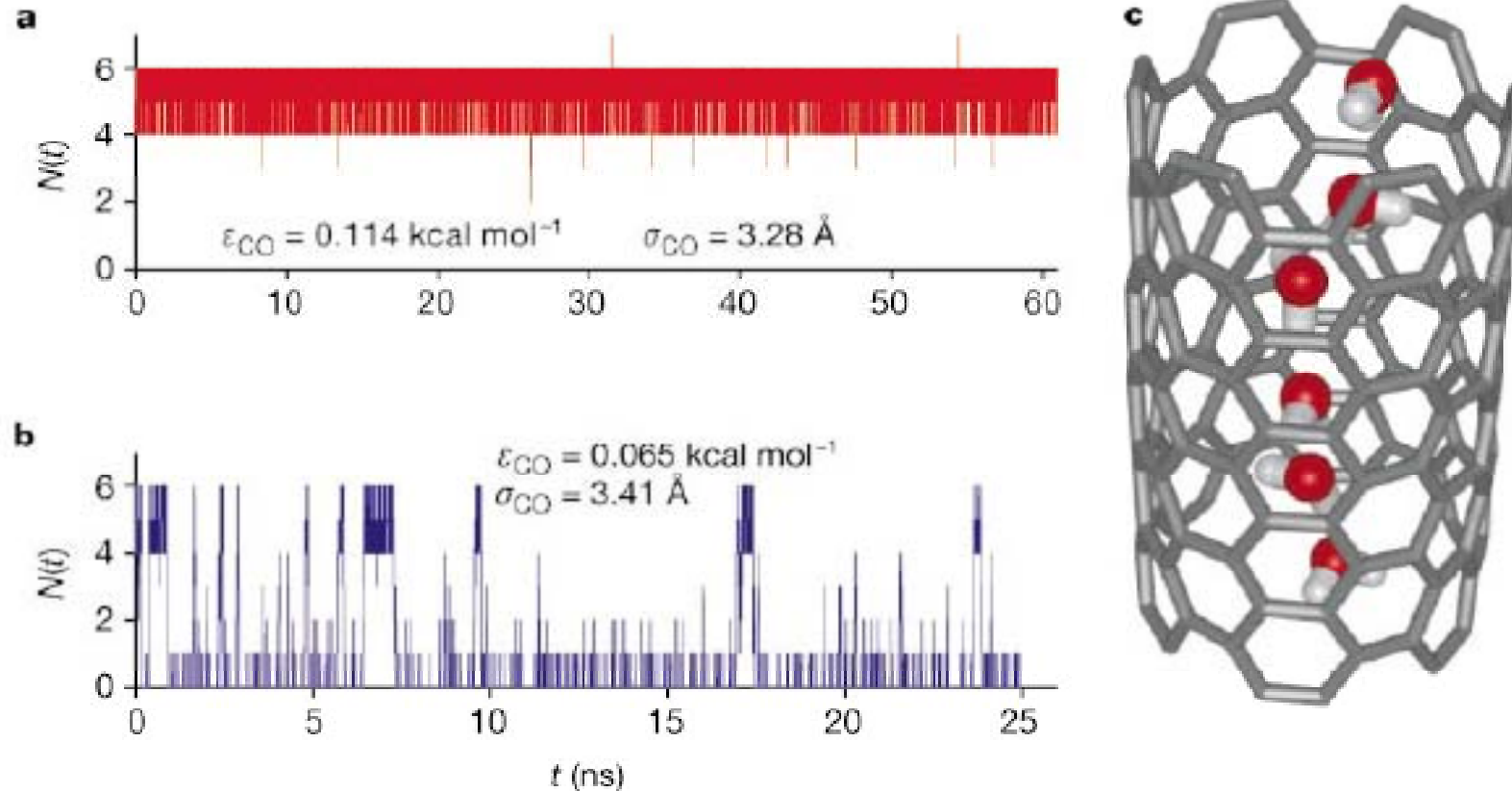
Nanofluidics??



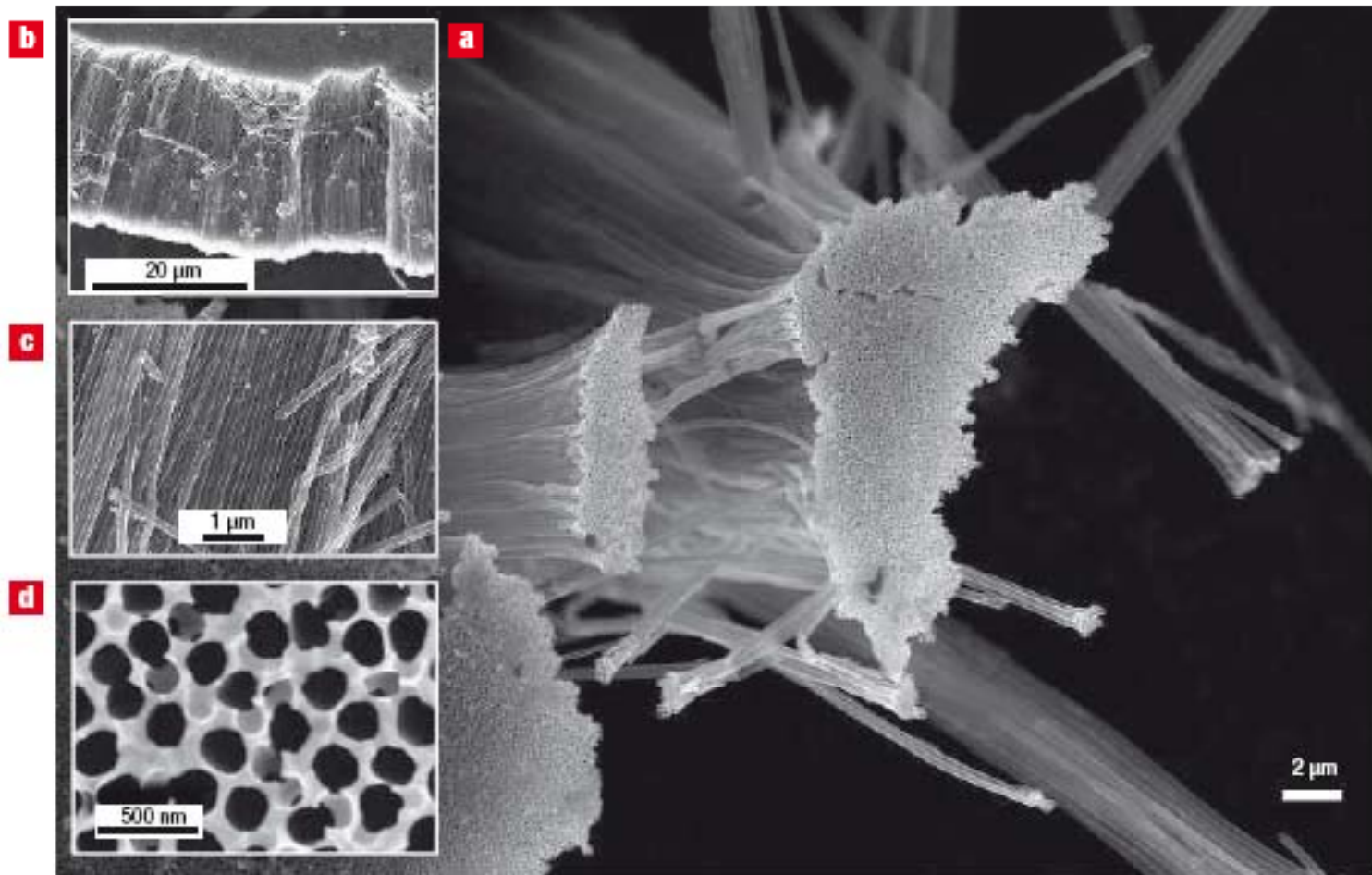
We plan to integrate a single single-walled carbon nanotube into a fluidic device in a way that fluid that is inserted through the inlet can reach the outlet only by flowing through the carbon nanotube. The image of the nanotube with simulated water molecules inside was taken from Hummer et al., Nature 414, 188.

<http://www.tudelft.nl/live/pagina.jsp?id=c88a0cb5-0ffa-4027-85bd-139f28a7e4fd&lang=en>

Case Study II: Nanotube Nanofluidics



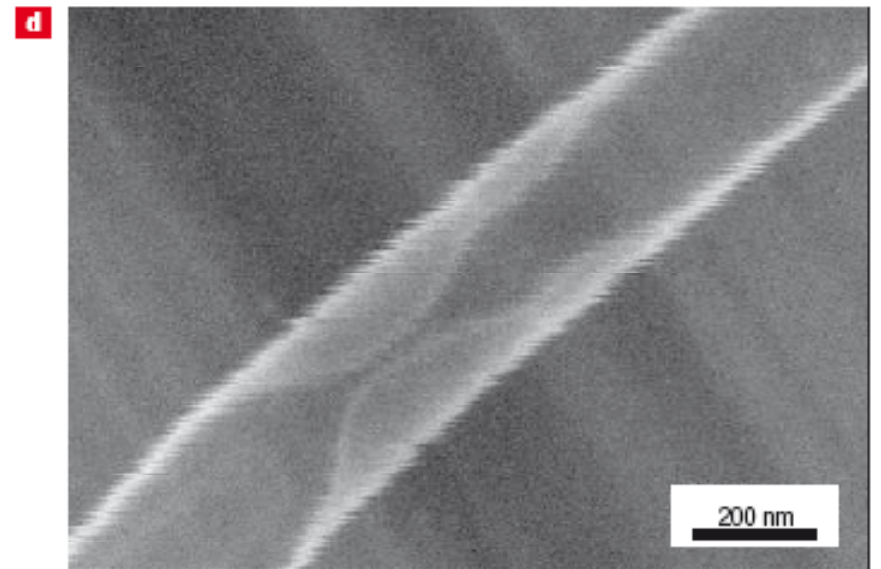
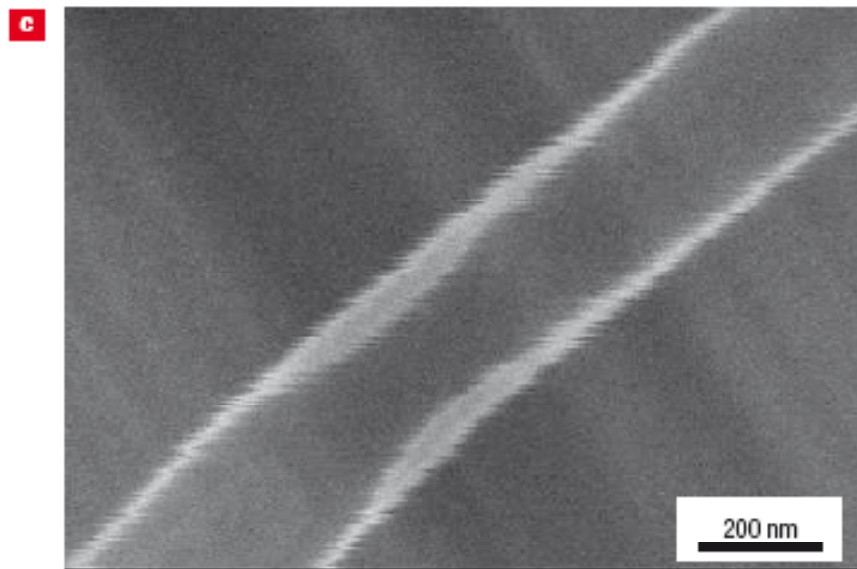
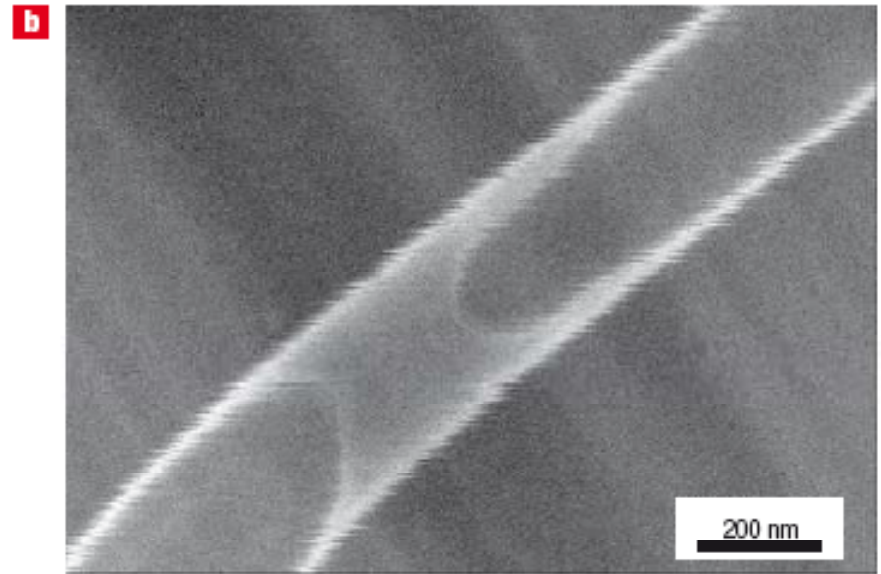
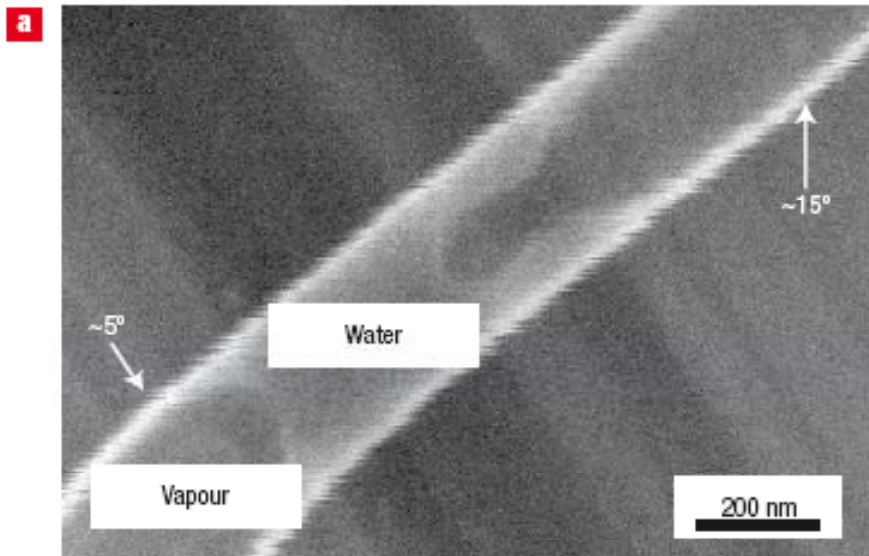
Water occupancy. a, b, Number N of water molecules inside the nanotube as a function of time for sp² carbon parameters (a) and reduced carbon±water attractions (b). c, Structure of the hydrogen-bonded water chain inside the nanotube.



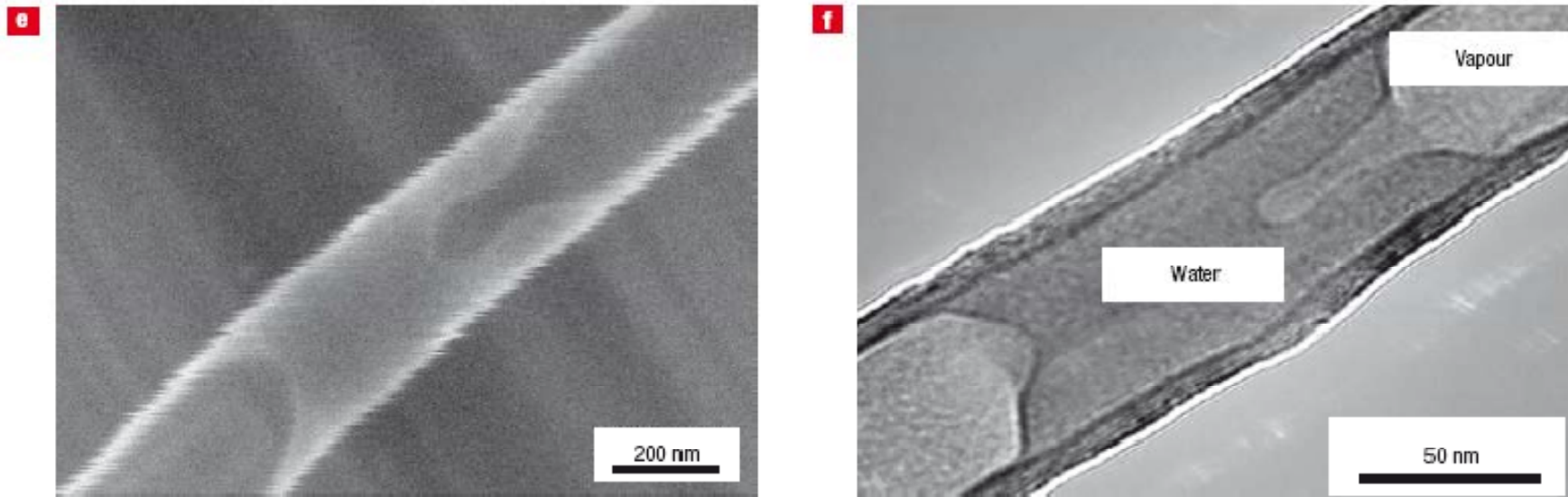
SEM images of carbon nanopipes produced by the authors using standard chemical vapour deposition. **a**, Nanopipes partially released from an anodic aluminium oxide template following sonication in NaOH. **b**, Cross section of intact carbon coated membrane. **c**, Higher magnification view of individual aligned carbon pipes. **d**, Surface of carbon membrane showing open pores (diameter ~ 160 nm).

nature nanotechnology, 2 87-94, 2007

Self-assembly and Nanotechnology

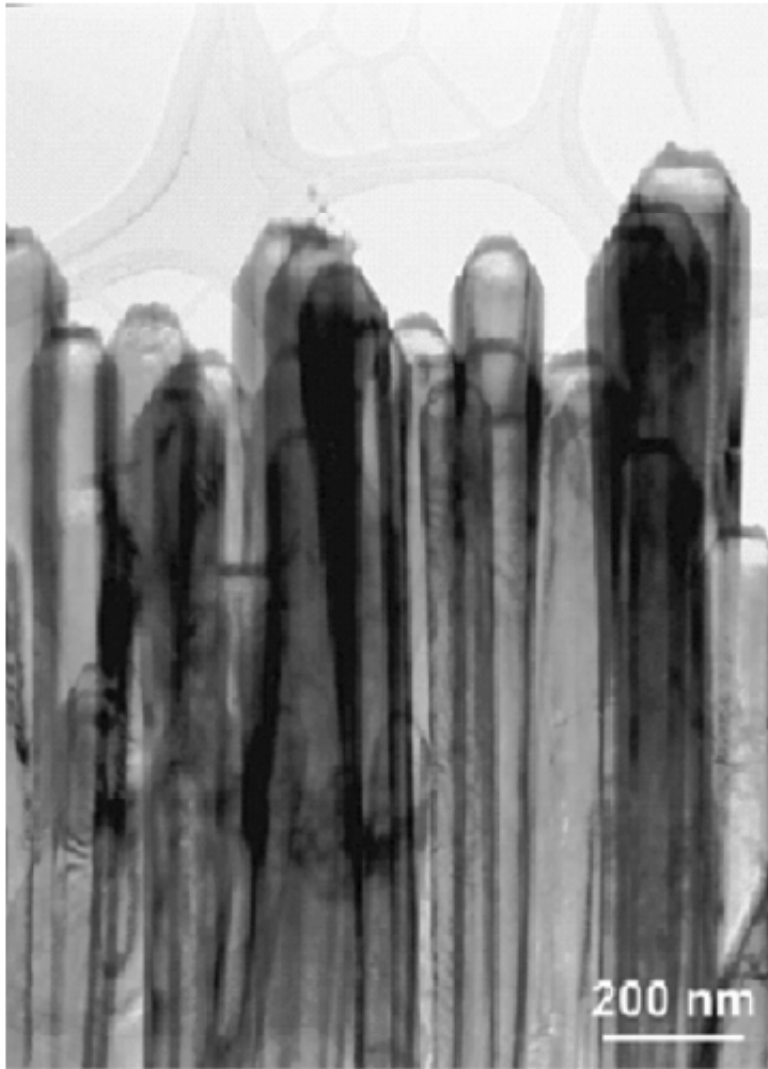


Dynamic behaviour of a water plug in a carbon nanopipe



ESEM images of the dynamic behaviour of a water plug in a carbon nanopipe. **a–e**, The meniscus shape changes when the stage temperature is constant but the vapour pressure of the water in the chamber is changed: **a**, 5.5 Torr, **b**, 5.8 Torr, **c**, 6.0 Torr, **d**, 5.8 Torr and **e**, 5.7 Torr (where the meniscus returns to the shape seen in **a**). The asymmetrical shape of the meniscus, especially the complex shape of the meniscus on the right side in **a** and **e** is a result of the difference in the vapour pressure caused by the open left end and closed right end of the tube. Estimated contact angles between the meniscus and the tube wall are indicated at two locations. **f**, TEM image showing a similar plug shape in a closed carbon nanotube under pressure.

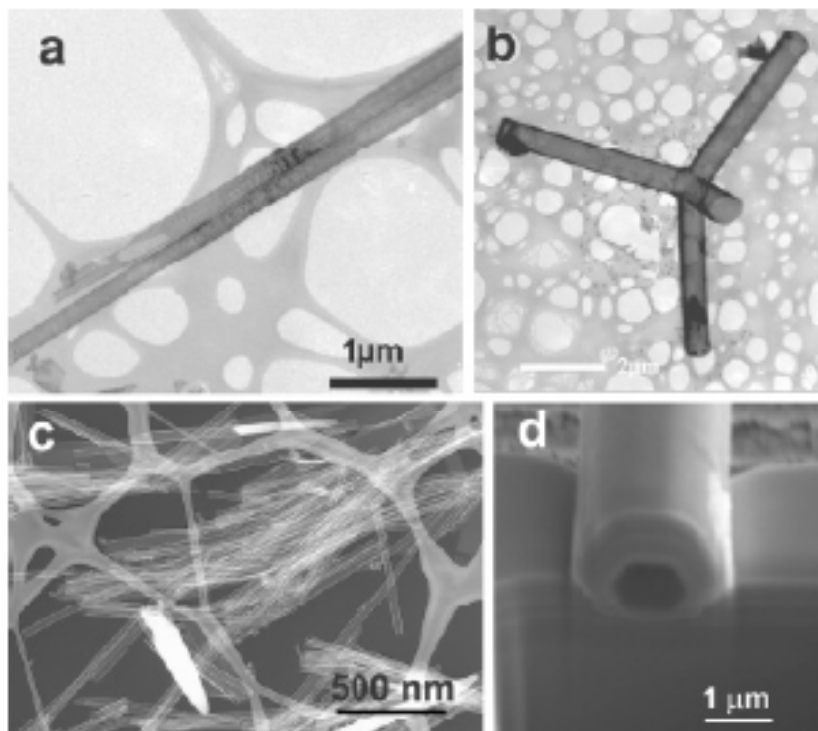
Nanotubes



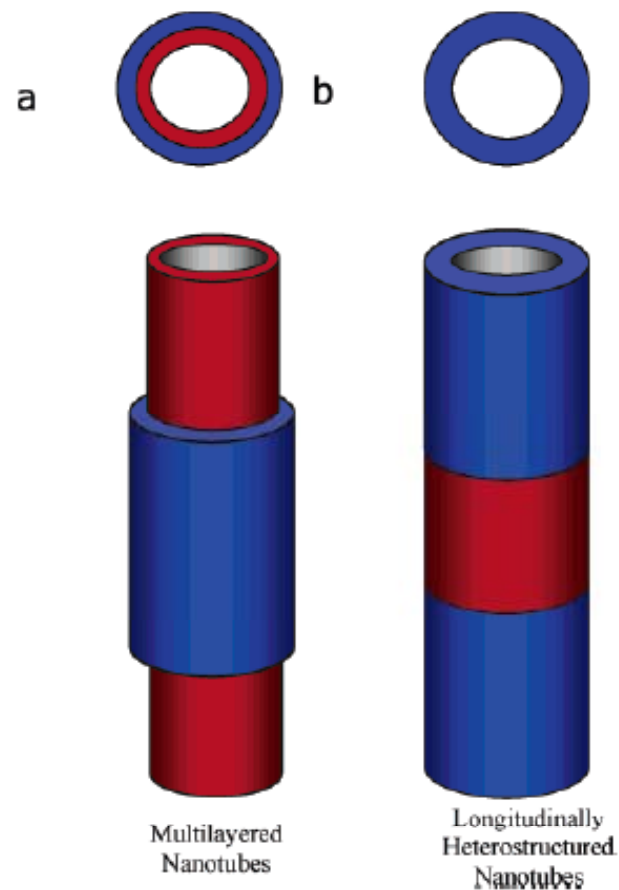
Transmission electron microscopy image of a cluster of single-crystalline GaN nanotubes prepared using the epitaxial casting methodology.

Annu. Rev. Mater. Res. 2004. 34:83–122

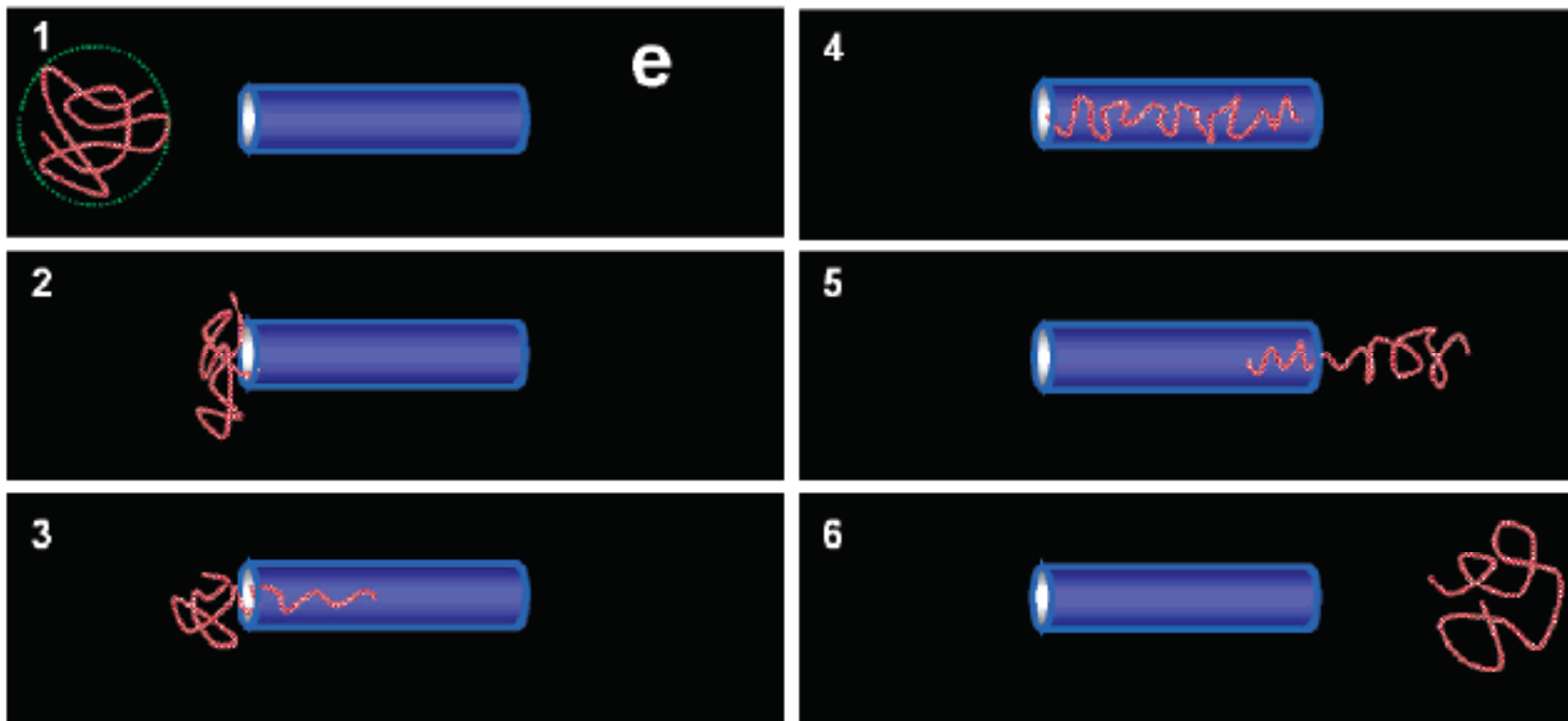
Nanotubes



SEM and TEM images of various nanotube materials that have been produced using nanowires as templates: (a) TEM micrograph of single-crystalline Mn-doped GaN nanotubes; (b) TEM image of branched silica nanotubes templated from ZnO tetrapods; (c) TEM image of amorphous TiO₂ nanotubes; (d) SEM micrograph of a multilayered Si/SiO₂ nanotube.



Schematic drawings (cross-sectional and perspective view) of several possible complex nanotube structures: (a) multilayered nanotubes; (b) longitudinal junctioned nanotubes.



Single DNA molecule detection in nanotubes. Panels a and b are ionic current signals for λ -DNA translocations at $[KCl] = 2\text{ M}$ and the statistics of current change and duration time. Panels c and d are data for experiments carried out at $[KCl] = 0.5\text{ M}$ (adapted from ref 50). Panel e shows a schematic illustration of DNA translocation through a long nanotube, in which a complex DNA conformational evolution is involved